Achievable Data Rate Analysis of Clipped Flip-OFDM in Optical Wireless Communication

Zhenhua Yu[1], Robert J. Baxley[2] and G. Tong Zhou[1]
[1] School of Electrical and Computer Engineering, Georgia Institute of Technology, Atlanta, Georgia 30332–0250, USA
[2] Georgia Tech Research Institute, Atlanta, GA 30332-0821, USA
Email: zhenhuayu@gatech.edu

***Abstract*—Optical wireless communication (OWC) systems employ simple low-cost intensity modulation and direct detection (IM/DD) techniques, which require that the electric signal must be real-valued and unipolar. Flip orthogonal frequency division multiplexing (Flip-OFDM) is one of the unipolar OFDM techniques developed for OWC. In this paper, we will analyze the clipping effects on Flip-OFDM and derive the achievable data rates under both average optical power and dynamic optical power constraints. Finally, the Flip-OFDM will be compared with the DC biased optical OFDM (DCO-OFDM).**

I. Introduction

Orthogonal frequency division multiplexing (OFDM) has been considered for optical wireless communication (OWC) thanks to its ability to boost data rates and efficiently combat inter-symbol-interference. In OWC, simple low-cost intensity modulation and direct detection (IM/DD) techniques are employed, which require that the electric signal must be real-valued and unipolar (positive-valued). Four methods have been discussed in the literature for creating real-valued unipolar OFDM signal for OWC: DC biased optical OFDM (DCO-OFDM) [1], Asymmetrically clipped optical OFDM (ACO-OFDM) [2], Flip-OFDM [3], [4], and Unipolar OFDM (U-OFDM) [5]. However, one disadvantage of OFDM is its high peak-to-average-power ratio (PAPR) due to the summation over a large number of terms. The OFDM signal often has to be double-sided clipped in order to fit the front-end power constraints, which meanwhile introduces nonlinear distortions. There are two power constraints in the transmitter of OWC. First, the dynamic range of electric signal is limited by the nonlinearity of light emitting diodes (LEDs) [6]. Second, the average optical power is constrained due to the limit on power consumption, eye safety regulation, dim illumination requirement, etc..

A number of papers [7], [8], [9] have analyzed the double-sided clipped DCO-OFDM and ACO-OFDM and compared their bit error rate (BER), achievable data rate, bandwidth efficiency, etc. It was shown in [9] that DCO-OFDM is advantageous than ACO-OFDM in term of the achievable data rate. However, the clipping effects on Flip-OFDM and U-OFDM have not been studied so far. In this paper, we will focus on the Flip-OFDM since U-OFDM is the same with Flip-OFDM except for the slight difference in transmission order of time-domain samples. We will derive the optimum clipping level and achievable data rates of clipped Flip-OFDM subject to both the average optical power and dynamic optical power constraints. Finally, we will compare the performance of Flip-OFDM with DCO-OFDM.

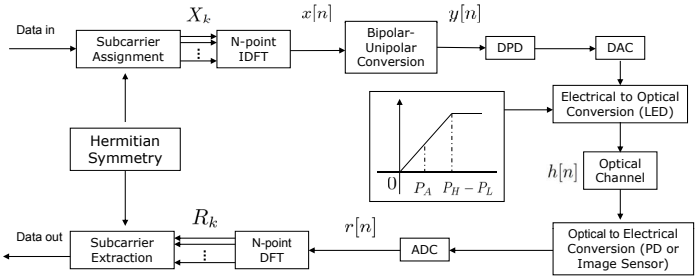

Fig. 1. OFDM system model in optical wireless communication

II. System model

A. Optical OFDM System

The optical OFDM system model discussed in this work is depicted in Fig. 1. In an OFDM system, a discrete time-domain signal $\mathbf{x} = [x[0], x[1], \ldots, x[N-1]]$ is generated by applying the inverse DFT (IDFT) operation to a frequency-domain signal $\mathbf{X} = [X_0, X_1, \ldots, X_{N-1}]$ as

$$x[n] = \text{IDFT}(X_k) = \frac{1}{\sqrt{N}} \sum_{k=0}^{N-1} X_k \exp(j2\pi kn/N), \qquad (1)$$

where $0 \le n \le N-1$, $j = \sqrt{-1}$ and N is the size of IDFT. In OWC, the IM/DD schemes require that the electric signal be real-valued and unipolar (positive-valued). According to the property of IDFT, a real-valued time-domain signal $x[n]$ corresponds to a frequency-domain signal X_k that is Hermitian symmetric; i.e.,

$$\begin{aligned} X_k &= X_{N-k}^*, \quad 1 \le k \le N-1, \\ X_k &\in \Re, \quad k = 0, N/2, \end{aligned} \qquad (2)$$

where $*$ denotes complex conjugate. X_0 and $X_{N/2}$ do not carry information and are generally set to zero. According to the Central Limit Theorem, $x[n]$ is approximately Gaussian distributed with zero mean and variance σ^2 with probability density function (pdf):

$$p(x) = \frac{1}{\sigma}\phi\left(\frac{x}{\sigma}\right), \qquad (3)$$

978-1-4673-4941-3/12/$31.00 ©2012 IEEE

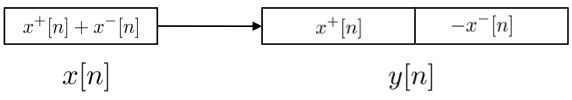

Fig. 2. Bipolar-unipolar conversion for Flip-OFDM

where $\phi(z)=\frac{1}{\sqrt{2\pi}}e^{-\frac{1}{2}z^2}$ is the pdf of the standard Gaussian distribution. As a result, the time-domain OFDM signal $x[n]$ tends to occupy a large dynamic range and is bipolar.

A unipolar signal $y[n]$ is obtained from $x[n]$ after some bipolar-unipolar conversion operations. The unipolar real-valued signal $y[n]$ is then converted to analog signal and subsequently modulate the intensity of the LED. In this paper, we assume that the digital pre-distortion (DPD) has perfectly linearized the LED between the interval $[P_L, P_H]$, where P_L is the turn-on voltage (TOV) for the LED. If the TOV is provided by an analog module at the LED and we assume that LED is already turned on, the linear range for the input signal is $[0, P_H - P_L]$. At the receiver, the photodiode, or the image sensor, converts the received optical signal to electrical signal and transforms it to digital form. The received sample can be expressed as

$$r[n] = y[n] \otimes h[n] + w[n], \tag{4}$$

where $h[n]$ is the impulse response of the wireless optical channel, $w[n]$ is additive white Gaussian noise (AWGN) with variance σ_w^2, and $\otimes$ denotes convolution. In this paper, we consider two widely used channel models in OWC: i) the AWGN channel: $h[n]=\delta[n]$; ii) the ceiling bounce channel model [10]: $h[n]=H(0)6a^6/(nT+a)^7u[n]$, where $H(0)$ is the gain constant, T denotes the sample interval, $a=12\sqrt{11/23}D$ and $u[n]$ is the unit step function. D denotes the rms delay.

B. Flip-OFDM

Fig. 2 shows the bipolar-unipolar conversion for Flip-OFDM. The unipolar signal $y[n]$ is composed of a positive part and a negative part from $x[n]$

$$x[n] = x^+[n] + x^-[n], \tag{5}$$

where the positive part $x^+[n]$ and the negative part $x^-[n]$ are obtained as

$$x^+[n] = \begin{cases} x[n], & x[n] > 0 \\ 0, & x[n] < 0 \end{cases} \tag{6}$$

$$x^-[n] = \begin{cases} x[n], & x[n] < 0 \\ 0, & x[n] > 0 \end{cases} \tag{7}$$

The positive component $x^+[n]$ is transmitted in the first frame, while the flipped negative component $-x^-[n]$ is transmitted in the second frame. Thus, all the samples in both frames are positive and real-valued.

At the receiver, assume the channel $h[n]$ is constant over two frames, the two received components can be expressed as

$$r^+[n] = x^+[n] \otimes h[n] + w^+[n], \tag{8}$$

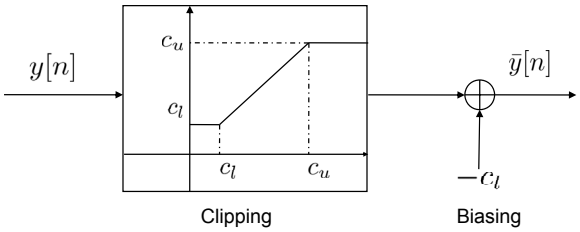

Fig. 3. Clipping and biasing model

$$r^-[n] = -x^-[n] \otimes h[n] + w^-[n], \tag{9}$$

where $w^+[n]$ denotes the Gaussian noise of the positive component and $w^-[n]$ denotes the Gaussian noise of the negative component, respectively. Then the bipolar signal is reconstructed as

$$\begin{aligned} r[n] &= r^+[n] - r^-[n] && (10)\\ &= (x^+[n] + x^-[n]) \otimes h[n] + w^+[n] + w^-[n] \\ &= x[n] \otimes h[n] + w^\star[n], && (11) \end{aligned}$$

where $w^\star[n] = w^+[n] + w^-[n]$ denotes the sum Gaussian noise which has the power $2\sigma_w^2$. With noise filtering scheme [11], for AWGN channel, the noise power can be further reduced by a factor $\beta \in (-3, 0)$ dB.

III. Achievable Data Rate Analysis

A. Clipping and Biasing Model

In order to fit the signal within the optical power constraints of the transmitter, a clipping and biasing model shown in Fig. 3 is used in [8], [9]. The output $\bar{y}[n]$ is obtained from $y[n]$ after clipping and biasing operations

$$\bar{y}[n] = \begin{cases} c_u - c_l, & y[n] > c_u \\ y[n] - c_l, & c_l \le x[n] \le c_u \\ 0, & x[n] < c_l \end{cases}, \tag{12}$$

where c_u denotes the upper clipping level, and c_l denotes the lower clipping level. To facilitate the analysis, we define the clipping ratio γ and the biasing ratio ς as

$$\gamma \triangleq \frac{(c_u - c_l)/2}{\sigma}, \quad \varsigma \triangleq \frac{-c_l}{c_u - c_l}. \tag{13}$$

Thus, the upper and lower clipping levels can be written as

$$c_u = 2\sigma\gamma(1-\varsigma), \quad c_l = -2\sigma\gamma\varsigma. \tag{14}$$

The ratios γ and ς can be adjusted independently causing c_u and c_l to vary. In an OWC system, the intensity of light emitted by the LED is proportional to $\bar{y}[n]$. In the optical communication literature, the average optical power of the LED input signal $\bar{y}[n]$ is defined as

$$O_{\bar{y}} \triangleq \mathcal{E}\{\bar{y}[n]\}, \tag{15}$$

where $\mathcal{E}[\cdot]$ denotes statistical expectation. Due to the limit on power consumption, eye safety regulation, dim illumination requirement, etc., the OWC system usually operates under some average optical power constraint P_A; i.e., $O_{\bar{y}} \le P_A$.

The OWC system is further limited by the dynamic range of the LED. We define the dynamic optical power of $\bar{y}[n]$ as

$$G_{\bar{y}} \triangleq \max\left(\bar{y}[n]\right) - \min\left(\bar{y}[n]\right). \tag{16}$$

$G_{\bar{y}}$ should be constrained by $P_H - P_L$ as $G_{\bar{y}} \leq P_H - P_L$. Moreover, $\bar{y}[n]$ must be nonnegative; i.e., $\bar{y}[n] \geq 0$.

We define the optical signal to noise ratio (OSNR) and the dynamic signal to noise ratio (DSNR) as

$$\text{OSNR} \triangleq \frac{O_{\bar{y}}}{\sigma_w}, \quad \text{DSNR} \triangleq \frac{G_{\bar{y}}}{\sigma_w}. \tag{17}$$

Let $\eta_{OSNR} = P_A/\sigma_w$ denote the OSNR constraint and $\eta_{DSNR} = (P_H - P_L)/\sigma_w$ denote the DSNR constraint. The ratio $\eta_{DSNR}/\eta_{OSNR} = (P_H - P_L)/P_A$ is determined by specific system requirements. We have

$$\frac{\sigma}{\sigma_w} \leq \frac{\eta_{OSNR}}{O_{\bar{y}}/\sigma}, \quad \frac{\sigma}{\sigma_w} \leq \frac{\eta_{DSNR}}{G_{\bar{y}}/\sigma}. \tag{18}$$

The maximum σ/σ_w value can be obtained as

$$\frac{\sigma}{\sigma_w} = \min\left(\frac{\eta_{OSNR}}{O_{\bar{y}}/\sigma}, \quad \frac{\eta_{DSNR}}{G_{\bar{y}}/\sigma}\right), \tag{19}$$

After the clipping and biasing, the two components of Flip-OFDM can be expressed as

$$\bar{x}^+[n] = \begin{cases} c_u - c_l, & x^+[n] > c_u \\ x^+[n] - c_l, & c_l \leq x^+[n] \leq c_u \\ 0, & x^+[n] < c_l \end{cases} \tag{20}$$

$$-\bar{x}^-[n] = \begin{cases} c_u - c_l, & -x^-[n] > c_u \\ -x^-[n] - c_l, & c_l \leq -x^-[n] \leq c_u \\ 0, & -x^-[n] < c_l \end{cases} \tag{21}$$

We can calculate the average optical power of $\bar{y}[n]$ as

$$\begin{aligned} O_{\bar{y}} &= \mathcal{E}\{\bar{y}[n]\} = \mathcal{E}\{\bar{x}^+[n]\} = \mathcal{E}\{-\bar{x}^-[n]\} \qquad (22)\\ &= \int_{c_l}^{c_u}(x-c_l)\frac{1}{\sigma}\phi\left(\frac{x}{\sigma}\right)dx + \int_{c_u}^{\infty}(c_u-c_l)\frac{1}{\sigma}\phi\left(\frac{x}{\sigma}\right)dx \\ &= \sigma\Big(\phi(2\gamma\varsigma) - \phi\left(2\gamma(1-\varsigma)\right) - 2\gamma\varsigma\Phi\left(-2\gamma\varsigma\right) \\ &\quad +2\gamma(1-\varsigma)\Phi\left(-2\gamma(1-\varsigma)\right) + 2\gamma\varsigma\Big), \end{aligned}$$

where $\Phi(x) = \int_{-\infty}^{x}\phi(t)dt$. We can obtain the dynamic optical power of $\bar{y}[n]$ as

$$G_{\bar{y}} = \max\left(\bar{y}[n]\right) - \min\left(\bar{y}[n]\right) = c_u - c_l = 2\sigma\gamma. \tag{23}$$

At the receiver, we can obtain the reconstructed signal

$$\bar{r}[n] = \bar{x}[n] \otimes h[n] + w^{\star}[n], \tag{24}$$

where

$$\begin{aligned} \bar{x}[n] &= \bar{x}^+[n] + \bar{x}^-[n] \qquad (25)\\ &= \begin{cases} c_u - c_l, & x[n] > c_u \\ x[n] - c_l, & c_l \leq x[n] \leq c_u \\ 0, & -c_l < x[n] < c_l \\ x[n] + c_l, & -c_u \leq x[n] \leq -c_l \\ c_l - c_u, & x[n] \leq -c_u \end{cases} \end{aligned}$$

B. Signal to Distortion Ratio

Based on the Bussgang's Theorem [12], any nonlinear function of $x[n]$ can be decomposed into a scaled version of $x[n]$ plus a distortion term $d[n]$ that is uncorrelated with $x[n]$. For example, we can write,

$$\bar{x}[n] = \alpha \cdot x[n] + d[n], \quad n = 0, \ldots, N-1. \tag{26}$$

Let $R_{xx}[m] = \mathcal{E}\{x[n]x[n+m]\}$ denote the auto-correlation function of $x[n]$, and let $R_{\bar{x}x}[m] = \mathcal{E}\{\bar{x}[n]x[n+m]\}$ denote the cross-correlation function between $\bar{x}[n]$ and $x[n]$ at lag m . For any given m, the correlation functions satisfy

$$R_{xd}[m] = 0, \quad R_{\bar{x}x}[m] = \alpha R_{xx}[m]. \tag{27}$$

Thus the scaling factor α can be calculated as

$$\begin{aligned} \alpha &= \frac{R_{\bar{x}x}[0]}{R_{xx}[0]} = \frac{\mathcal{E}\{\bar{x}[n]x[n]\}}{\sigma^2} \qquad (28)\\ &= \frac{1}{\sigma^2}\int_{-\infty}^{\infty}\bar{x}x\cdot p(x)dx \\ &= \frac{2}{\sigma^2}\Big(\int_{c_l}^{c_u}(x-c_l)x\frac{1}{\sigma}\phi\left(\frac{x}{\sigma}\right)dx \\ &\quad +\int_{c_u}^{\infty}(c_u-c_l)x\frac{1}{\sigma}\phi\left(\frac{x}{\sigma}\right)dz\Big) \\ &= 2\Phi\left(2\gamma(1-\varsigma)\right) - 2\Phi\left(-2\gamma\varsigma\right). \end{aligned}$$

Note that in (28) we have used Eq. (14) for c_l and c_u. It is shown in reference [13] that the output auto-correlation function $R_{\bar{x}\bar{x}}[m]$ is related to the input auto-correlation function $R_{xx}[m]$ via

$$R_{\bar{x}\bar{x}}[m] = \sum_{\ell=0}^{\infty}\frac{b_\ell^2}{\ell!}\left[\frac{R_{xx}[m]}{\sigma^2}\right]^{\ell}, \tag{29}$$

where the coefficients

$$b_\ell = \frac{(-1)^\ell\sigma^{\ell-1}}{\sqrt{2\pi}}\int_{-\infty}^{\infty}\bar{x}\frac{d^\ell[\exp(-\frac{x^2}{2\sigma^2})]}{dx^\ell}dx. \tag{30}$$

From Eq. (25) and Eq. (30), we can obtain the coefficient b_ℓ as a function of the clipping ratio γ and the biasing ratio ς:
i) $\ell = 1$

$$b_1 = 2\sigma\Phi\left(2\gamma(1-\varsigma)\right) - 2\sigma\Phi(-2\gamma\varsigma), \tag{31}$$

ii) $\ell > 1$ and is odd

$$\begin{aligned} b_\ell &= \frac{2\sigma}{\sqrt{2\pi}}\exp\left(-2\gamma^2\varsigma^2\right)He_{(\ell-2)}\left(-2\gamma\varsigma\right) - \qquad (32)\\ &\quad \frac{2\sigma}{\sqrt{2\pi}}\exp\left(-2\gamma^2(1-\varsigma)^2\right)He_{(\ell-2)}\left(2\gamma(1-\varsigma)\right), \end{aligned}$$

iii) ℓ is even

$$b_\ell = 0, \tag{33}$$

where $He_n(t) = (-1)^\ell\exp\left(\frac{t^2}{2}\right)\frac{d^\ell[\exp(-\frac{t^2}{2})]}{dt^\ell}$ is the probabilists' Hermite polynomials [14].

Fig. 4 shows the framework for signal to distortion ratio (SDR) calculation. The input auto-correlation function $R_{xx}[m]$

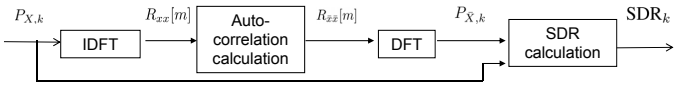

Fig. 4. Framework for signal to distortion (SDR) calculation

can be obtained from taking IDFT of the input power spectrum density (PSD)

$$R_{xx}[m] = \text{IDFT}\{P_{X,k}\}_m, \quad m = 0, \ldots, N-1, \tag{34}$$

where $P_{X,k} = \mathcal{E}[|X_k|^2]$ is the expected value of the power on the kth subcarrier before clipping. Then it is straightforward to calculate the output PSD by taking the DFT of the auto-correlation of the output signal:

$$P_{\bar{X},k} = \text{DFT}\{R_{\bar{x}\bar{x}}[m]\}_k, \quad k = 0, \ldots, N-1. \tag{35}$$

Taking the DFT of the Eq. (26), the data at the kth subcarrier is expressed as

$$\begin{aligned} \bar{X}_k &= \text{DFT}\{\alpha \cdot x[n]\}_k + \text{DFT}\{d[n]\}_k \\ &= \alpha \cdot X_k + D_k, \quad k = 0, \ldots, N-1. \end{aligned} \tag{36}$$

The SDR at the kth subcarrier is given by

$$\text{SDR}_k = \frac{\mathcal{E}[|\alpha \cdot X_k|^2]}{\mathcal{E}[|D_k|^2]} = \frac{\alpha^2 P_{X,k}}{P_{D,k}} = \frac{\alpha^2 P_{X,k}}{P_{\bar{X},k} - \alpha^2 P_{X,k}}, \tag{37}$$

where $P_{D,k} = \mathcal{E}[|D_k|^2] = P_{\bar{X},k} - \alpha^2 P_{X,k}$ is the average power of the distortion on the kth subcarrier.

C. Achievable Data Rate

By taking the DFT of Eq. (24), we can obtain the received data on the kth subcarrier as

$$\begin{aligned} \bar{R}_k &= H_k \bar{X}_k + W_k^\star \\ &= \alpha H_k X_k + H_k D_k + W_k^\star. \end{aligned} \tag{38}$$

The signal-to-noise-and-distortion ratio (SNDR) for the kth subcarrier is given by

$$\begin{aligned} \text{SNDR}_k &= \frac{|H_k|^2 \alpha^2 \mathcal{E}\{|X_k|^2\}}{|H_k|^2 \mathcal{E}\{|D_k|^2\} + \mathcal{E}\{|W_k^\star|^2\}} \\ &= \frac{|H_k|^2 \alpha^2 P_{X,k}}{|H_k|^2 P_{D,k} + 2\beta\sigma_w^2} \\ &= \left(\text{SDR}_k^{-1} + \frac{2\beta\sigma_w^2}{\alpha^2 |H_k|^2 P_{X,k}} \right)^{-1}. \end{aligned} \tag{39}$$

In this paper, we assume the power is equally distributed on all information-bearing subcarriers; i.e., $P_{X,k} = N\sigma^2/(N-2)$. Then Eq. (39) is reduced to

$$\text{SNDR}_k = \left(\text{SDR}_k^{-1} + \frac{\sigma_w^2}{\sigma^2} \cdot \frac{2\beta(N-2)}{N\alpha^2 |H_k|^2} \right)^{-1}. \tag{40}$$

By substituting Eq. (19) into Eq. (40), we obtain the SNDR at the kth subcarrier:

$$\begin{aligned} \text{SNDR}_k &= \left((\text{SDR}_k)^{-1} + \frac{2\beta(N-2)}{N\alpha^2 |H_k|^2} \right. \\ &\qquad \left. \cdot \max\left(\frac{O_{\bar{y}}^2/\sigma^2}{\eta_{OSNR}^2}, \quad \frac{G_{\bar{y}}^2/\sigma^2}{\eta_{DSNR}^2} \right) \right)^{-1}. \end{aligned} \tag{41}$$

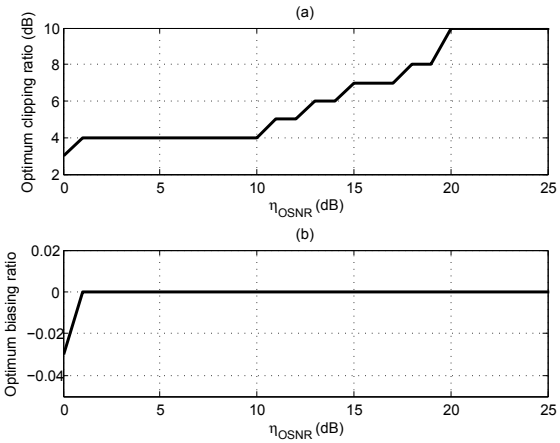

Fig. 5. Optimal clipping ratio and biasing ratio for $\eta_{DSNR}/\eta_{OSNR} = 18$ dB, and AWGN channel.

Therefore, the achievable data rate, as a function of γ, ς, η_{OSNR}, η_{DSNR}, and channel response, is given by

$$\begin{aligned} &\mathcal{R}(\gamma, \varsigma, \eta_{OSNR}, \eta_{DSNR}, \mathbf{H}) \\ &= \frac{1}{2N} \sum_{k=1}^{N/2-1} \log_2(1 + \text{SNDR}_k) \frac{\text{bits}}{\text{subcarrier}}. \end{aligned} \tag{42}$$

For given η_{OSNR}, η_{DSNR} values and channel response $\mathbf{H}$, we can obtain a pair of optimum clipping ratio $\gamma^\ddagger$ and optimum biasing ratio $\varsigma^\ddagger$ that maximize the achievable data rate by

$$(\gamma^\ddagger, \varsigma^\ddagger) = \underset{(\gamma,\varsigma)}{\text{argmax}} \quad \mathcal{R}|_{\eta_{OSNR}, \eta_{DSNR}, \mathbf{H}}, \tag{43}$$

and the corresponding achievable data rate.

IV. Numerical Results

In this section, we show numerical results of achievable data rate for clipped Flip-OFDM under various average optical power and dynamic optical power constraints and compare it with DCO-OFDM. The number of subcarriers was $N = 512$. For the AWGN channel, we assumed the best performance $\beta = -3$ dB can be achieved for all SNR scenarios. For the ceiling-bounce channel model, we chose the rms delay spread $D = 10$ ns and sampling frequency 100 MHz.

As examples, we chose $\eta_{DSNR}/\eta_{OSNR} = 18$ dB, and the channel was AWGN. Fig. 5 shows the optimal clipping ratio and optimum biasing ratio as a function of η_{OSNR}. We can observe that with a higher average optical power constraint, the clipping ratio can be increased to achieve higher data rates and clipping the bottom for the purpose of reducing the average optical power is unnecessary ($\varsigma^\ddagger = 0$). Intuitively, when η_{OSNR} is large, the channel noise has little effect and the clipping distortion dominates. Next, we chose the ratio η_{DSNR}/η_{OSNR} from 6dB, 18dB and no η_{DSNR} constraints. For each pair of η_{OSNR}, η_{DSNR}, AWGN channel or ceiling-bounce channel, we can calculate the optimum clipping ratio $\gamma^\ddagger$ and biasing ratio $\varsigma^\ddagger$ according to Eq. (43) and the corresponding achievable data rates. Fig. 6, Fig. 7, and Fig. 8 show the achievable data

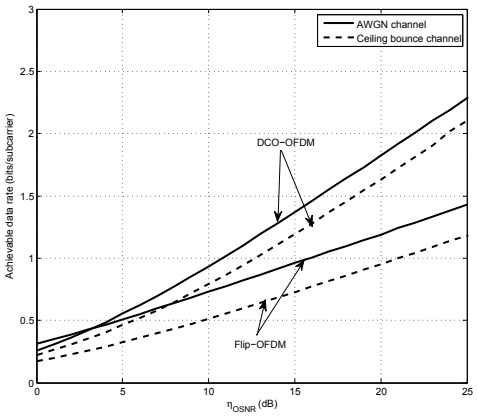

Fig. 6. Achievable data rate with optimal clipping ratio and optimal biasing ratio for $\eta_{OSNR} = 0, 1, ..., 25$ dB (in step size of 1 dB), and $\eta_{DSNR}/\eta_{OSNR} = 6$ dB.

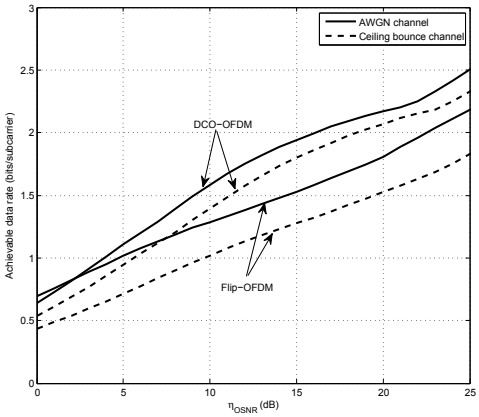

Fig. 7. Achievable data rate with optimal clipping ratio and biasing ratio for $\eta_{OSNR} = 0, 1, ..., 25$ dB (in step size of 1 dB), and $\eta_{DSNR}/\eta_{OSNR} = 18$ dB.

rates with optimal clipping ratio and biasing ratio for the case $\eta_{DSNR}/\eta_{OSNR} = 6$ dB, $\eta_{DSNR}/\eta_{OSNR} = 18$ dB, and no η_{DSNR} constraint, respectively. The achievable data rate of DCO-OFDM [9] was plotted as well to be compared with Flip-OFDM. We observe that the performance of Flip-OFDM and DCO-OFDM depends on the specific optical power constraints scenario. Generally, DCO-OFDM outperforms Flip-OFDM for all the cases. With the increase of the ratio η_{DSNR}/η_{OSNR}, the average optical power becomes the dominant constraint. The Flip-OFDM moves closer to the DCO-OFDM. For the no η_{DSNR} constraint case, which is practically impossible, Flip-OFDM become better than DCO-OFDM when $\eta_{OSNR} > 20$ dB.

V. Conclusion

The achievable data rate of clipped Flip-OFDM was derived in this paper. We investigated the trade-off between the optical power constraint and distortion. We analyzed the optimum clipping ratio and biasing ratio and compared the performance

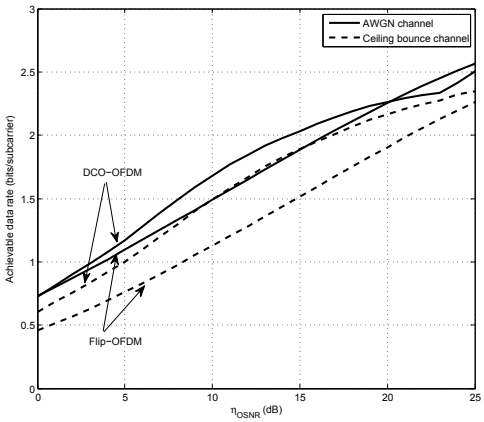

Fig. 8. Achievable data rate with optimal clipping ratio and biasing ratio for $\eta_{OSNR} = 0, 1, ..., 25$ dB (in step size of 1 dB), and no η_{DSNR} constraint.

of Flip-OFDM and DCO-OFDM techniques. Numerical results showed that DCO-OFDM outperforms the Flip-OFDM for most of the optical power constraint scenarios.

Acknowledgment

This work was supported in part by the Texas Instrument DSP Leadership University Program.

References

[1] S. Hranilovic, "On the design of bandwidth efficient signalling for indoor wireless optical channels," *International Journal of Communication Systems*, vol. 18, no. 3, pp. 205–228, 2005.

[2] J. Armstrong and A. J. Lowery, "Power efficient optical OFDM," *Electronics Letters*, vol. 42, no. 6, pp. 370–372, 2006.

[3] J. Yong, "Modulation and demodulation apparatuses and method for wired / wireless communication," Korea Patent WO2007/064 165 A, 2007.

[4] N. Fernando, Y. Hong, and E. Viterbo, "Flip-OFDM for optical wireless communications," in *Proc. IEEE Information Theory Workshop*. IEEE, 2011, pp. 5–9.

[5] D. Tsonev, S. Sinanovic, and H. Haas, "Novel unipolar orthogonal frequency division multiplexing (U-OFDM) for optical wireless communication," in *Proc. IEEE VTC 2012-Spring*, 2012, to appear.

[6] T. Kamalakis, J. Walewski, G. Ntogari, and G. Mileounis, "Empirical volterra-series modeling of commercial light-emitting diodes," *Journal of Lightwave Technology*, no. 99, 2011.

[7] R. Mesleh, H. Elgala, and H. Haas, "On the performance of different ofdm based optical wireless communication systems," *Journal of Optical Communications and Networking*, vol. 3, no. 8, pp. 620–628, 2011.

[8] S. Dimitrov, S. Sinanovic, and H. Haas, "A comparison of OFDM-based modulation schemes for OWC with clipping distortion," in *Proc. IEEE GLOBECOM Workshop on OWC*, Dec. 2011, pp. 787 –791.

[9] Z. Yu, R. J. Baxley, and G. T. Zhou, "EVM and achievable data rate analysis of clipped OFDM signals in visible light communication," *EURASIP Journal on Wireless Communications and Networking*, submitted for publication.

[10] J. Kahn and J. Barry, "Wireless infrared communications," *Proceedings of the IEEE*, vol. 85, no. 2, pp. 265–298, 1997.

[11] N. Fernando, Y. Hong, and E. Viterbo, "Flip-OFDM for unipolar communication systems," *Arxiv preprint arXiv:1112.0057*, 2011.

[12] J. Bussgang, "Crosscorrelation functions of amplitude-distorted gaussian signals," *NeuroReport*, vol. 17, no. 2, 1952.

[13] W. Davenport and W. Root, *An introduction to the theory of random signals and noise*. IEEE Press, 1987.

[14] M. Abramowitz and I. Stegun, *Handbook of mathematical functions with formulas, graphs, and mathematical tables*. Dover publications, 1964, vol. 55, no. 1972.